In situ Detection Of Free And Trapped Electrons In Dye-Sensitized Solar Cells By Photo-Induced Microwave Reflectance Measurements

Halina K. Dunn[1,1], Laurence M. Peter[1,],Stephen J. Bingham[2], Eric Maluta[2,2] and Alison B. Walker[2]*

1. Department of Chemistry, University of Bath, Bath BA2 7AY, UK

2. Department of Physics, University of Bath, Bath BA2 7AY, UK

Keywords. complex permittivity, intensity-modulated, mobility, waveguide

Received Date:

* corresponding author: email: l.m.peter@bath.ac.ukk

[1] Current address: Department of Chemistry, Ludwig Maximilian University, Butenandtstrasse 11, 81377 Munich, Germany.

[2] Current address: Physics Department, University of Venda, P/Bag X5050, Thohoyandou 0950, South Africa.

ABSTRACT

In order to study the behavior of photoinjected electrons in dye-sensitized solar cells (DSC), steady-state microwave reflectance measurements (33 GHz, Ka band) have been carried out on a working cell filled with electrolyte. The experimental arrangement allowed simultaneous measurement of the light-induced changes in microwave reflectance and open circuit voltage as a function of illumination intensity. In addition, frequency-resolved intensity-modulated microwave reflectance measurements were used to characterize the relaxation of the electron concentration at open circuit by interfacial transfer to tri-iodide ions in the electrolyte. The dependence of the free and trapped electron concentrations on open circuit voltage were derived respectively from conductivity data (obtained by impedance spectroscopy) and from light-induced near IR transmittance changes. These electron concentrations were used in the fitting of the of the microwave reflectivity response, with electron mobility as the main variable. Changes in the complex permittivity of the mesoporous films were calculated using Drude-Zener theory for free electrons and a simple harmonic oscillator model for trapped electrons. Comparison of the calculated microwave reflectance changes with the experimental data showed that the experimental response arises primarily from the perturbation of the real component of the complex permittivity by the high concentration of trapped electrons present in the DSC under illumination. The results suggest that caution is needed when interpreting the results of microwave reflectance measurements on materials with high concentrations of electron (or hole) traps, since an *a priori* assumption that the microwave response is solely determined by changes in conductivity (i.e. by free electrons) may be incorrect. The intensity-modulated microwave reflectance measurements showed that relaxation of the free and trapped electron concentrations occurs on a similar time scale, confirming that the free and trapped electron populations remain in quasi-equilibrium during the decay of the electron concentration.

INTRODUCTION

Dye-sensitized solar cells are an interesting alternative to conventional p-n junction devices, and they have been studied intensively[1] since their original development by O'Regan and Grätzel.[2] Their operation has been reviewed elsewhere,[3,4] but a brief summary is as follows. Efficient light harvesting in the DSC is achieved by a layer of sensitizer dye adsorbed on the high internal surface area of a mesoporous TiO_2 film. Photoexcitation of the dye leads to rapid electron injection into the conduction band of the oxide, leaving the dye in its oxidized state. Following electron injection, the dye is regenerated by electron transfer from iodide ions in the liquid electrolyte that permeates the mesoporous TiO_2 layer. Finally, the tri-iodide ions formed in the regeneration step diffuse through the electrolyte to the cathode, where they are reduced to iodide ions to complete the cycle.

Microwave reflectance methods, including the time-resolved microwave conductivity (TRMC) technique, have been applied to the characterization of many different semiconductor materials,[5-7] as well as in the study of electrochemical[8-15] and solid state junctions.[16] More recently, TRMC has been employed to investigate organic photovoltaic systems[17] and mesoporous films of TiO_2 (bare and sensitized) in the absence of electrolyte and conducting substrate.[18-20] In these previous studies, the mesoporous TiO_2 layers were not in contact with a redox electrolyte, which is an essential component of the DSC. However, Friedrich and Kunst[21] used a quasi solid-state DSC with thin 'dry' film of iodide/tri-iodide left behind by evaporation of the solvent, and Salafsky et al.[22] studied dye-sensitized TiO_2 particles suspended in an electrolyte.

The objective of the present study was to use the microwave reflectance technique to probe changes in the complex permittivity of the TiO_2 film, brought about by injection of electrons from the sensitizing dye, in a working electrolyte-filled DSC under illumination. In a normal semiconductor sample, the light-induced change in permittivity arises from the creation of electron hole-pairs. However, in the DSC, the change in permittivity of the TiO_2 arises from electron injection from the

photoexcited sensitizer dye. In this case, the 'hole' is the I_3^- ion (in the following discussion we assume that any changes in the microwave permittivity of the electrolyte are negligible).

Electrons in the TiO_2 film may behave differently in electrolyte-filled DSCs compared with dry TiO_2 films. The value of making measurements on complete DSCs rather than on dry sensitized TiO_2 films is illustrated by recent simultaneous *in situ* time-resolved measurements of current, voltage and optical absorbance.[23] A key issue, as far as microwave reflectance measurements are concerned, is that the position of the electron quasi Fermi level relative to the redox Fermi level can be controlled and measured (as a photovoltage) in an electrolyte-filled DSC. This is not possible in an isolated film. In the measurements described in this paper, a specially designed DSC was mounted on the end of the microwave waveguide as shown in Figure 1. The conducting fluorine-doped tin oxide layer was removed in the center section, as shown, in order to eliminate reflection effects arising from the substrate. This design enabled simultaneous measurement of the microwave reflectivity and the open circuit voltage (via the contacted area outside the waveguide cross section).

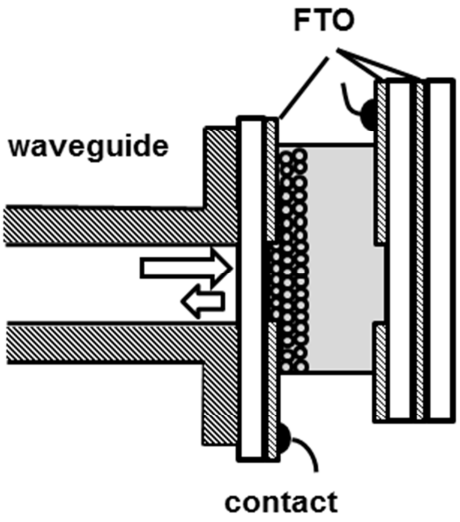

Figure 1. Cross-section view (not to scale) of a dye-sensitized solar cell mounted on the end of the microwave waveguide. A rectangular area with dimensions 3.5 × 7.0 mm^2 of the fluorine-doped tin oxide (FTO) layer is removed on both sides of the cell to prevent problems with microwave reflection.

A striking difference between DSCs and conventional photovoltaic devices is the fact that most of the electrons present in the DSC under operating conditions are localized in electron traps in the band gap of the TiO_2.[24-26] The existence of a broad exponential trap distribution in mesoporous TiO_2 films - with typical trap densities exceeding 10^{24} m^{-3} - has been deduced from charge extraction[27,28] and near IR absorbance measurements.[29-31] The electron trap density scales with the surface area of the TiO_2 particles in the mesoporous film.[32,33] This suggests that the traps are associated with surface defects or with electrostatic interactions of electrons with ions in the electrolyte, which typically has a concentration in excess of 10^{26} m^{-3}. The transient and periodic voltage/current responses of DSCs to time-dependent perturbations are strongly influenced by the dynamic exchange of electrons between traps and the conduction band.[34] By contrast, the dc photocurrent and photovoltage are determined only by the behavior of free electrons, because the rates of electron trapping and detrapping are equal under steady state conditions.

It is often assumed that the microwave reflectance method probes light-induced changes in conductivity, i.e. changes in the imaginary component of the permittivity. For high quality bulk materials like silicon, light-induced changes in microwave reflectance are indeed dominated by the change in conductivity of the sample.[5] However, time-resolved microwave studies of nanocrystalline titania (TiO_2) show that photoexcitation can also lead to large changes in the real component of the complex permittivity.[35,36] For example Kytin et al.[35] have reported UV-induced changes in the real component of the microwave permittivity of 6 nm and 16 nm anatase particles that are comparable in magnitude to the changes in the imaginary component. Trapped electrons may also contribute to the light-induced microwave reflectance response of compound semiconductors[37] or materials such as nanocrystalline films[35,38] and polymers.[39]

The influence of trapped electrons on the microwave permittivity of semiconductors such as CdS has been considered by Hartwig and Hinds[40] and more recently by Grabtchak and Cocivera.[37] We have used their approach to interpret microwave reflectance measurements on working dye-sensitized solar cells (DSCs). Calculation of the contribution of free electrons requires values of the free electron

conductivity (determined by the mobility and concentration of free electrons) as a function of open circuit voltage. These values were deduced from the impedance response of the DSC. Calculation of the contribution of trapped electrons requires information about the density, energetic distribution and population of electron traps. This information was obtained from near-IR absorbance measurements.[30] The results show that the light-induced microwave response is strongly influenced by changes in the concentration of trapped electrons. This conclusion is important, since it may have implications for the interpretation of microwave reflectance measurements on other disordered systems with traps, such as bulk heterojunction solar cells, a subject of considerable current interest.

THEORY

Illumination of the DSC changes the complex relative permittivity, ε_r, of the TiO_2 film

$$\varepsilon_r = \varepsilon_r^{'} - i\varepsilon_r^{''} = \varepsilon_r^{'} - i\frac{\sigma}{\varepsilon_0 \omega} \tag{1}$$

where ω is the microwave angular frequency and ε_0 is the vacuum permittivity. The normalized light-induced change in microwave reflectance ΔR_M can be written in the general form

$$\frac{\Delta R_M}{R_M} = \frac{R_M\left(\varepsilon_r + \Delta\varepsilon_r\right) - R_M\left(\varepsilon_r\right)}{R_M\left(\varepsilon_r\right)} \tag{2}$$

where $R_M(\varepsilon_r)$ is the reflectance in the dark, ε_r is the relative permittivity in the dark and $\Delta\varepsilon_r$ is the light-induced change in relative permittivity. It is often assumed that ΔR_M is dominated by changes in conductivity, σ, associated with increases in free electron concentration under illumination, so that the ε and $\Delta\varepsilon$ terms in equation 2 are replaced by σ and $\Delta\sigma$ respectively. Here, we make no such assumption. Instead, we calculate ΔR_M from the total light-induced change in relative permittivity, which can be divided into a contribution $\delta\varepsilon_{free}$ due to perturbation of the free electron concentration, δn_c, and a contribution $\delta\varepsilon_{tr}$ due to perturbation of the trapped electron concentration, δn_t. Thus

$$\delta\varepsilon_r = \delta\varepsilon_{free} + \delta\varepsilon_{tr} \tag{3}$$

Perturbation of the permittivity due to changes in free electron concentration

The conductivity of the mesoporous TiO_2 layer in the DSC is very low in the dark because the electron Fermi level is pinned to the I_3^-/I^- redox Fermi level, which is typically at least 0.8 eV below the conduction band energy level.[41] The equilibrium free electron concentration, n_0, is given by

$$n_0 = N_C \, \mathrm{e}^{-\left(\frac{E_C - E_{F,redox}}{k_B T}\right)} \tag{4}$$

where E_C is the conduction band energy, $E_{F,redox}$ is the redox Fermi energy and N_C is the conduction band density of states, which depends of the effective electron mass, m^*.

$$N_C = 2\left[\frac{2\pi m^* k_B T}{h^2}\right]^{3/2} \tag{5}$$

For $m^*/m_e = 1$, $N_C = 2.49 \times 10^{25}$ m^{-3} at 298K. Estimates of $E_C - E_{F,redox}$ are typically of the order of 0.8 – 1.0 eV[41], corresponding to n_0 values between 7×10^{11} m^{-3} and 3×10^{8} m^{-3}.

The free electron concentration in the DSC increases by many orders of magnitude under illumination at open circuit since the electron quasi Fermi level is now higher by qV_{oc}, where V_{oc} is the open circuit voltage. In the non-degenerate case,

$$\frac{n_c}{n_0} = e^{\frac{qV_{oc}}{k_B T}} \tag{6}$$

where n_c is the concentration of free electrons under illumination. It follows that the conductivity of the TiO_2 film under illumination due to the free electrons is

$$\sigma = q\mu n_c = q\mu n_0 e^{\frac{qV_{oc}}{k_B T}} = \sigma_0 e^{\frac{qV_{oc}}{k_B T}} \tag{7}$$

where μ is the electron mobility and σ_0 is the dark conductivity. As shown below, the conductivity under illumination can be calculated from the electron transport resistance, which is obtained by measuring the open circuit electrical impedance as a function of frequency.

Grabtchak and Cocivera[37] use the Drude-Zener expression for the response to a time-dependent electric field with an angular frequency ω, $\delta\sigma = (\Delta n_c q^2\tau/m^*)/(1+i\omega\tau)$ to obtain

$$\delta\varepsilon_{free}' = -\frac{\delta n_c q^2\tau^2}{\varepsilon_0 m^*\left[1+(\omega\tau)^2\right]} \quad \delta\varepsilon_{free}'' = \frac{\delta n_c q^2\tau}{\varepsilon_0 m^*\omega\left[1+(\omega\tau)^2\right]} \tag{8}$$

Here m^* is the effective electron mass, ω is the microwave angular frequency and τ is the momentum relaxation time, which is related to the effective electron mass and μ by $\tau = m^*\mu/q$. τ is a measure of the linewidth of the response of the sample to the microwave radiation, which peaks at a characteristic frequency. The negative sign in the expression for $\delta\varepsilon_{free}'$ comes from screening of external fields by free electrons. At this point we note that the description of dielectric properties of nanocrystalline porous films is complicated by the effects of carrier localization in particles[35] and by local field effects.[42] These problems have been discussed recently by Nemec at al.[43] in the context of THz measurements on a range of materials. Here we limit the treatment of free electrons to the simple Drude model.

Calculations based on equations 8 show that the perturbation of the imaginary component of ε by free electrons is much larger than the change in the real component, confirming that the microwave response should be related primarily to changes in the conductivity of the sample, *provided that only free electrons are considered*. Figure 2a illustrates the predicted relationship between the perturbation of the complex dielectric constant of the TiO_2 and the open circuit voltage and conductivity. In order to enable subsequent comparison with the microwave reflectance data presented in the experimental section, we have used the values of electron mobility μ (10^{-5} m^2 V^{-1} s^{-1}) and $E_c - E_{F,redox}$ (0.85 eV) obtained by fitting the microwave reflectance results. Plots for other values of the electron mobility are given in the Supporting Information. The calculation confirms that $|\delta\varepsilon_{free}''| >> |\delta\varepsilon_{free}'|$ in the case of free electrons. The slopes of the semi-logarithmic plots for $|\delta\varepsilon_{free}''|$ and $|\delta\varepsilon_{free}'|$ vs. V_{oc} are $q/(2.303k_BT) = 16.8$ V^{-1}.

Reflectance Calculations

In order to calculate the microwave reflectance change brought about by the increase in electron concentration under illumination, the DSC is represented as a series of dielectric layers that terminate the waveguide (see Supporting Information). The spacings in the experimental configuration and the position of the short were chosen to optimize the microwave reflectance signal (see Supporting Information). We have demonstrated the utility of the dielectric stack approach previously in microwave reflectance studies of the silicon/electrolyte interface.[11,13,14] The reflectance is calculated using values of the relative permittivity of the TiO_2 layer corresponding to dark and illuminated conditions (the permittivity values for the other components of the cell are given in Table 1 below). Calculation details are given in the Supporting Information.

Material	ε'	ε''
glass[44]	6.82	0.049
TiO_2 (dark)[45]	12.0	0
electrolyte[46]	20.0	13.0
FTO[47]	12.0	3.5×10^4

Table 1. Values of relative microwave permittivity used in the reflectance calculations.

Figure 2b illustrates the magnitude of the corresponding light-induced microwave reflectance change arising from free electrons, calculated for the experimental DSC configuration. It can be seen that the semilogarithmic plot of $|\Delta R_M/R_M|$ vs. open circuit voltage for free electrons also has a slope of 16.8 $V^{-1.}$

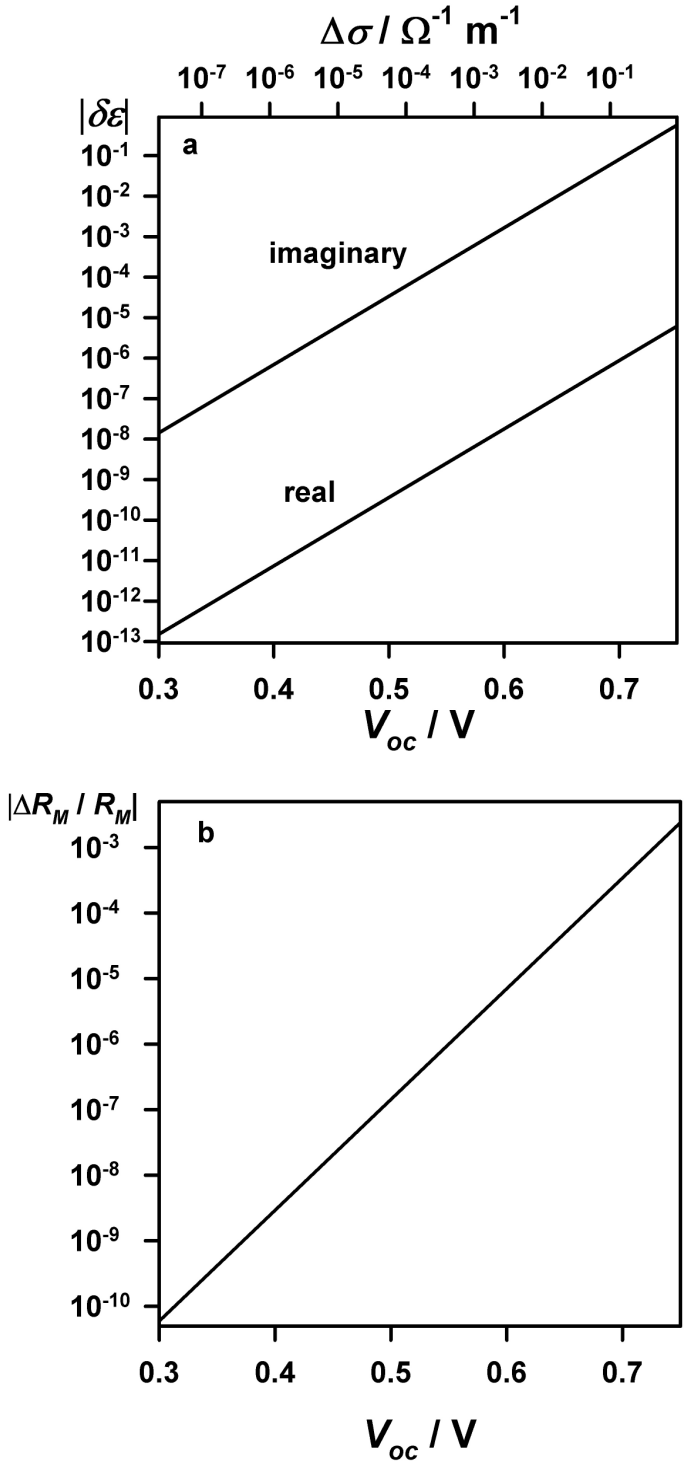

Figure 2. a). Changes in the magnitude of the real and imaginary parts of the complex relative permittivity of TiO_2 due to the increase in free electron concentration brought about by illumination of a DSC. Calculated as a function of open circuit voltage V_{oc}, with $\mu = 10^{-5}$ m^2 V^{-1} s^{-1}, $m^*/m_e = 1$, $E_C - E_{F,redox} = 0.85$ eV (section IV.1), $T = 298$K, and $\omega/(2\pi) = 33$ GHz. b). Corresponding normalized microwave reflectance change (free electrons) calculated for the experimental configuration used in this study using the values of $\delta\varepsilon_{free}'$ and $\delta\varepsilon_{free}''$ shown in Fig 2a. See Table 1 for permittivity values and Supporting Information for further details. The calculated reflectance change is negative for the stack configuration used.

Perturbation of the permittivity due to changes in trapped electron concentration

Hartwig and Hinds[40] were the first to develop a harmonic oscillator model to derive the influence of trapped electrons on the complex permittivity of semiconductors. Here, we follow the closely related approach of Grabtchak and Cocivera,[37] who have given expressions for the changes in the real and imaginary parts of the complex permittivity that arise from trapped electrons. The trapped electron is assumed to be an oscillator of characteristic frequency ω_0, whose restoring force is proportional to the electron displacement and whose binding energy is the trap depth, E_T. As shown in the Supporting Information, equating the kinetic energy of the orbiting electron with the Coulomb energy of the trap, gives ω_0^2 as

$$\omega_0^{\,2} = \frac{2}{m^*}\frac{\left(4\pi\varepsilon_0\right)^2}{q^4}E_T^3 \tag{9}$$

The changes in real and imaginary parts of ε_r at microwave frequencies are related to the change in trapped electron concentration, $\mathrm{d}n_t$, by the expressions

$$\mathrm{d}\delta\varepsilon_{tr}' = \frac{\mathrm{d}n_t q^2(\omega_0^2-\omega^2)}{\varepsilon_0 m^*\left[\left(\omega_0^2-\omega^2\right)^2+\omega^2/\tau^2\right]},\ \mathrm{d}\delta\varepsilon_{tr}'' = \frac{\mathrm{d}n_t q^2\omega}{\varepsilon_0 m^*\tau\left[\left(\omega_0^2-\omega^2\right)^2+\omega^2/\tau^2\right]} \tag{10}$$

In this model, τ has the same value for free and trapped electrons, since in both cases it is due to scattering, which takes place on a faster time scale than the oscillation period for trapped electrons. Unlike the free electron response, $\delta\varepsilon_{tr}'$ is positive because the trapped electrons increase the amount of polarizable charge.

Under illumination at open circuit, the increment in concentration of trapped electrons, $\mathrm{d}n_t$, in the energy interval E_T to $E_T + \mathrm{d}E_T$, is given by the product of the Fermi Dirac distribution $f_{FD}(E_T)$ and the trap distribution $g(E_T)$. For an exponential trap distribution, it follows that

$$\frac{\mathrm{d}n_t}{\mathrm{d}E_T} = \frac{\left(N_{T,0}/(k_B T_0)\right)\exp\left\{-\dfrac{(E_C-E_T)}{k_B T_0}\right\}}{1+\exp\left\{\dfrac{E_T-{}_nE_F}{k_B T}\right\}} \tag{11}$$

where $N_{T,0}$ is the total trap concentration and T_0 is an effective temperature describing the trap distribution. The perturbation of ε_r by trapped electrons is found by integrating the product of the derivatives in equations 10 and 11 over the energy range $E_{F,redox}$ to E_C. Figure 3 illustrates the dependence on trap depth of these two derivatives.

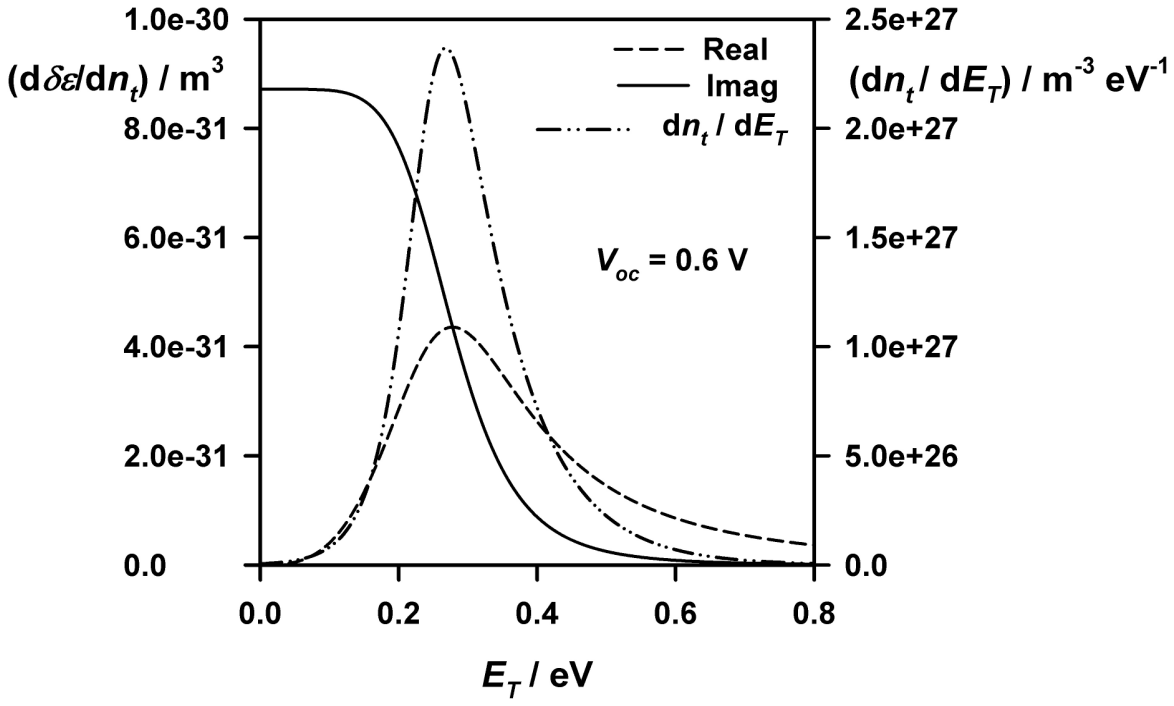

Figure 3. Plots showing the derivatives that describe the contribution of trapped electrons to the perturbation of the real and imaginary components of the complex microwave permittivity for an open circuit voltage V_{oc} = 0.6 V. The distribution of trapped electrons as a function of trap depth is also shown. $E_c - E_{F,redox}$ = 0.85 V, m^*/m_e = 1, $\mu = 10^{-5}$ m^2 V^{-1} s^{-1}, T_0 = 993 K, $N_{T,0} = 6.6 \times 10^{24}$ m^{-3}.

Figure 4a illustrates the changes in the complex relative permittivity of the TiO_2 film calculated for the trap distribution parameters used for Figure 3 and the same electron mobility (10^{-5} m^2 V^{-1} s^{-1}) used for Figure 2a. Figure 4b illustrates the corresponding change in microwave reflectance calculated for the same cell configuration as used for Figure 2b. In the case of the trapped electron distribution considered (T_0 = 993 K), the slope of the linear region of the semi-logarithmic reflectance plot has a slope of 12.5 V^{-1}.

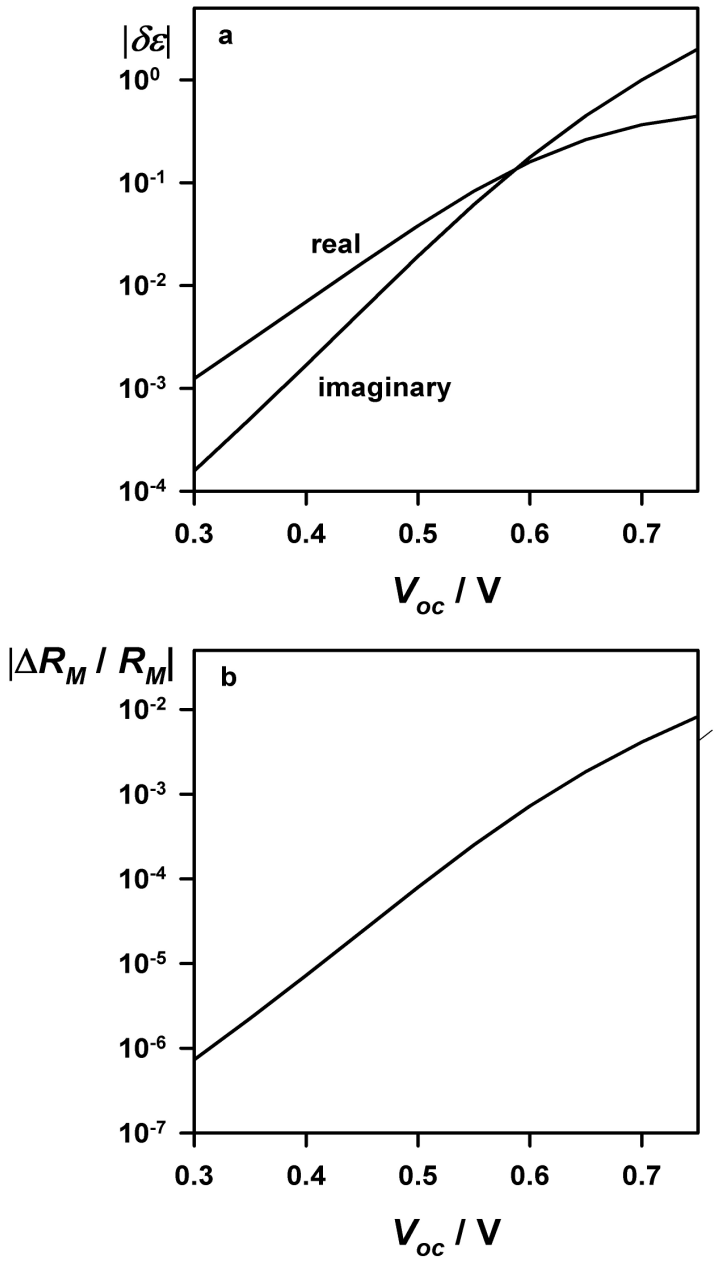

Figure 4.
a) Changes in the real and imaginary parts of the complex relative permittivity of TiO2 due to the increase in trapped electron concentration brought about by illumination of a DSC (δε' and δε" are both positive). Calculated as a function of open circuit voltage Voc for the experimentally measured trap distribution (see Fig 6) where NT,0 = 6.61 × 1024 m-3, T0 = 993 K . Other parameter values not related to trapped electrons are the same as for Figure 2.
b) Corresponding change in normalized microwave reflectance change (trapped electrons). Calculated for the experimental DSC configuration using the values of $\delta\varepsilon'$ and $\delta\varepsilon''$ shown in a). Other parameter values not related to trapped electrons are the same as for Figure 2.

In practice, $\Delta R_M/R_M$ should be determined by the total perturbation of the permittivity due to both free and trapped electrons. Comparison of Figures 2a and 4a shows that if the harmonic oscillator model

is applicable to the electrons in the DSC, we may expect the changes in relative permittivity (and hence in $\Delta R_M/R_M$) to be dominated by changes in the trapped electron concentration, particularly at low open circuit voltages. Consequently, since $T_0 > T$, the slope of the semilogarithmic plot of $\Delta R_M/R_M$ should be substantially lower than the 16.8 V^{-1} predicted for free electrons.

EXPERIMENTAL

The conducting glass (fluorine-doped tin oxide (FTO) Asahi glass, 10 ohm square, 1mm thick) used to fabricate the DSC reflects microwaves. Therefore, rectangular FTO-free windows corresponding to the cross section of the Ka-band waveguide were etched by masking off the desired area (3.5 x 7 mm) with Kapton tape and covering the exposed FTO with zinc granules (-30+100 mesh) and 36% HCl. This cell design, which is illustrated in Figure 1, allows measurement of the open circuit voltage whilst eliminating spurious microwave reflectance effects due to electron accumulation in the FTO when the DSC is illuminated. After cleaning the glass and applying a thin compact blocking layer of TiO_2 by spray pyrolysis of a 0.2 M solution of titanium(IV) isopropoxide, a one-centimeter square TiO_2 layer was deposited by doctor blading Dyesol DSL 18NR-T titania paste and heating to 500^{o}C for 30 minutes in air to remove the organic components. The resulting film thickness measured by profilometry was 13 μm. The same etching procedure was used to remove a corresponding rectangular area of FTO from the cathodes, which were coated with a thin platinum layer by thermal decomposition of chloroplatinic acid.

After sensitization of the TiO_2 film in a 0.5 mM solution of di-tetrabutylammonium cis-bis(isothiocyanato) bis(2,2'-bipyridyl-4,4'-dicarboxylato) ruthenium(II) (N719) in acetonitrile:tert-butanol overnight, the anode and cathode were sealed together using a 30 μm Surlyn spacer, taking particular care to ensure correct alignment of the two microwave transparent windows. Electrolyte (0.5 M LiI, 0.05 M I_2, 0.5 M tert-butylpyridine in 3-methoxyproipionitrile) was introduced via pre-drilled holes in the counter electrode, and an additional Asahi FTO glass sheet was used to seal the cell. This acts as a short, and was found to enhance the detected signal.

A schematic diagram of the K_a-band microwave set up (rectangular waveguide with inner dimensions 3.5 x 7 mm) is given in the Supporting Information, which also considers the minor effects of non-ideal termination of the waveguide. The geometry of the DSC terminating the waveguide was optimized to give the best possible microwave response by adjusting the thickness of the glass layers and the position of the FTO layer on glass that acts as a microwave short. Details are given in the Supporting Information. The microwave source was a 33 GHz Gunn diode (Atlantic Microwaves) protected by an isolator. The cell was mounted directly on the end of the waveguide, and the reflected microwaves were sampled using a directional coupler (coupling factor 7.5%) and a R422C crystal detector (Agilent technologies). The cell was enclosed in a box made of microwave-absorbent foam to minimize stray microwave reflections. A fiber optic of diameter 1 mm was used to introduce light onto the cell from a 530 nm continuous-wave laser, the intensity of which was adjusted using neutral density filters. In order to improve the signal/noise ratio of the detected microwave signal, the incident microwave power was square-wave modulated at 33 kHz using a PIN diode switch (Atlantic Microwaves) driven by the TTL output of a lock-in amplifier (Stanford Research Instruments SR 830 DSP). A Stanford Research Instruments SR 560 low noise preamplifier was used to amplify the signal from the crystal detector before detection by the lock in amplifier. The dark microwave reflectance of the cell was offset using a stabilized voltage source. The output of the lock-in amplifier was recorded on a Tektronix TDS 3012 digital storage oscilloscope (DSO), capable of averaging up to 512 frames. A TTL pulse generator was used to gate the laser and to trigger the DSO. Since the area of the etched windows was smaller than the area of the sensitized TiO_2 film, both the photovoltage and the photoconductivity could be monitored simultaneously. The photovoltage was monitored by the second channel of the DSO using a high impedance voltage follower. Depending on the signal strength, 5-30 transients were averaged for each measurement. The pulse length and repetition rate were adjusted to take into account the dependence of the rise and fall times on illumination intensity.

Impedance measurements were made at open circuit under illumination as a function of illumination intensity (and hence of open circuit voltage) using a potentiostat

(IVIUMSTAT.XR Electrochemical Interface). The cells were constructed in the same way as those used for the microwave reflectance study except that the FTO layers were not etched. Illumination was provided by a light-emitting diode (LED: Thorlabs, 627 nm), and the intensity was controlled using neutral density filters (Thorlabs). The cell was biased at the open circuit potential, and impedance spectra were recorded between 10^{-2} and 10^{5} Hz. Parameters related to the cathode and substrate were obtained by carrying out EIS on blank cells under applied bias in the dark. The impedance response was fitted using ZView (Scribner Associates) and the transmission line equivalent circuit developed by Bisquert and co-workers.[48] Details are given in the Supporting Information.

Trapped electron concentrations were measured using a near-IR absorbance method described elsewhere.[30] The optical cross-section of electrons at 950 nm was taken to be 5.4×10^{-22} m^2. [30] IMVS measurements were made using a standard setup.[49] Light-modulated microwave reflectance measurements[50] were carried out using a lock in amplifier and 100% depth modulation (setup shown in Supporting Information).

RESULTS AND DISCUSSION

Calculation of the perturbation of the permittivity by free electrons

In order to calculate the microwave response due to free electrons from equations 8, it is necessary to determine the value of δn_c, which determines the change in conductivity of the anatase film (equation 7). The conductivity is obtained by analyzing the open circuit impedance response of the illuminated DSC. The mesoporous oxide film is modeled as a transmission line with elements representing electron transport, electron transfer to the redox system and the chemical capacitance associated with electron storage in traps.[48] Details of the equivalent circuit and fitting are given in the Supporting Information. The cells used for the microwave measurements cannot be used for impedance measurements, which require the cell to be contacted over the entire TiO_2 film. Therefore the transport resistance R_{trans} was obtained as a function of open circuit voltage by fitting the impedance response of a nominally identical

DSC in which the conducting substrate was left intact. The conductivity, σ, of the free electrons in the TiO_2 film in the illuminated DSC was calculated from the relationship[49]

$$R_{trans} = \frac{d_{film}}{\sigma A} = \frac{d_{film}}{q n_c \mu A} \tag{12}$$

where d_{film} is thickness of the TiO_2 film (for simplicity, we ignore the effect of porosity), A is the area (1 cm^2). As we shall see, the key parameter that is varied to fit the microwave reflectance data is the electron mobility, μ. For any given value of μ, equation 7 is used to obtain n_c as a function of open circuit voltage from the fit shown in Figure 5. It is important to note that if μ and m^* are fixed and n_c is known, the value of $E_c - E_{F,redox}$ is fixed by equation 4 - 6.

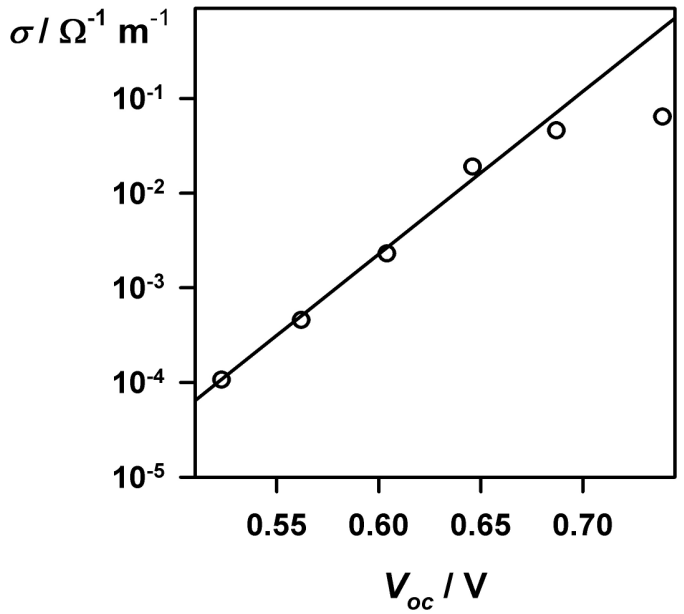

Figure 5. Variation of the conductivity of TiO_2 in an illuminated DSC measured by impedance spectroscopy as a function of open circuit voltage. The line shows a fit to equation 7 with the dark conductivity $\sigma_0 = 1.1 \times 10^{-13}$ Ω^{-1} m^{-1}, $T = 293$K.

The semilogarithmic plot in Figure 5 shows that the experimental variation of the conductivity agrees with the dependence of free electron concentration on open circuit voltage given for the non-degenerate case by equations 4 and 7, with a slope of 16.8 V^{-1}. The flattening observed at high open circuit voltages has been observed in previous work.[51,52] It may be an artifact arising from difficulties in obtaining a reliable fit for low values of R_{trans} due to overlap with the impedance semicircle arising from

the cathode. For the purposes of the present discussion it suffices to note that the dependence of free electron concentration on V_{oc} is ideal up to nearly 0.7V

For given values of electron mobility, the perturbation of the relative permittivity of the TiO_2 associated with free electrons was calculated as follows using the fit in Figure 5. First, the effective mass of electrons m^*/m_e was taken to be unity based on the work of Tang et al.,[53] and the corresponding value of N_C was calculated (there is some uncertainty about the effective mass of electrons in anatase,[54-56] but the value of m^* has little influence on the calculated reflectance change). Next, the value of $E_C - E_{F,redox}$ was obtained from equations 4 - 7 using the conductivity fit shown in Figure 5. Then the light-induced perturbations of the real and imaginary parts of the permittivity of the TiO_2 (cf. Figure 2a) were calculated from equations 8. Finally, the corresponding changes in microwave reflectivity illustrated in Figure 2 were calculated using the dielectric stack model of the DSC. This procedure was used in the fitting of the experimental microwave data, which involved varying the electron mobility to obtain the best match of the microwave reflectance as a function of open circuit voltage.

Calculation of the perturbation of the permittivity by trapped electrons

Figure 6 illustrates the variation of the measured trapped electron concentration with open circuit voltage. The data were fitted to an exponential trap distribution with a characteristic temperature T_0 = 993 K. The values of $N_{T,0}$ and $E_C - E_{F,redox}$ given in the figure caption are those obtained in the fitting of the microwave results by varying the electron mobility as described above. The electron trap distribution obtained by fitting the near absorbance data was used to calculate $\delta\varepsilon_t$ and $\Delta R_M/R_M$ for trapped electrons as a function of open circuit voltage as shown in Figures 4a and 4b

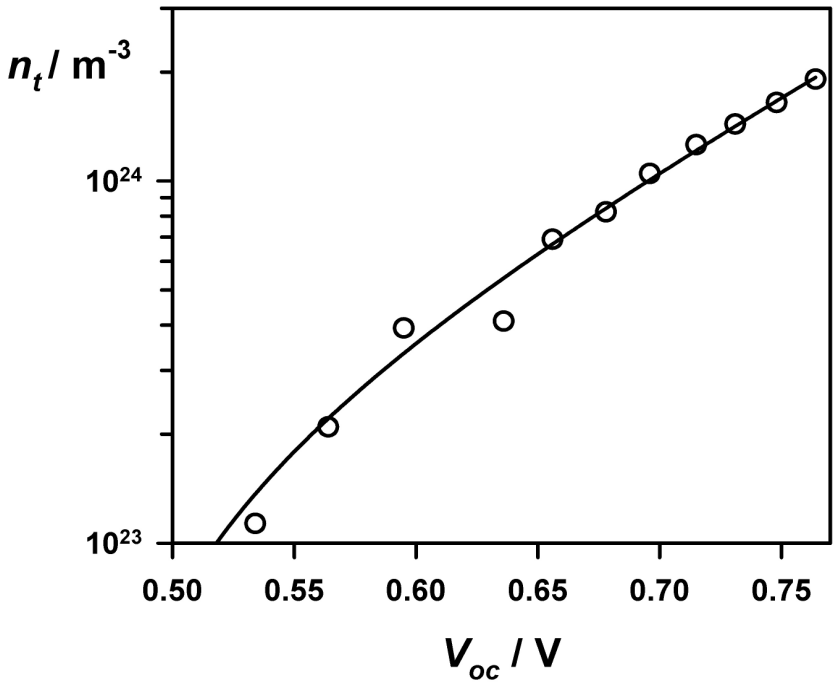

Figure 6. Trapped electron concentration as a function of open circuit voltage measured by near-IR absorbance. The fit shown is for an exponential trap energy distribution with a characteristic temperature of 993 K. $N_{T,0} = 6.61 \times 10^{24}$ m^{-3}, $E_C - E_{F,redox} = 0.85$ V.

Fitting the experimental microwave response

Figure 7 illustrates the simultaneous recording of the microwave reflectance and the open circuit voltage responses to slowly chopped illumination. The initial photovoltage is not zero because the voltage decay is very slow. The reason for this is that decay of the electron concentration by transfer of electrons from the substrate to tri-iodide ions [57,58] is negligible because the FTO has been etched away in the window area and a blocking layer was used in the surrounding area. The pulse length and off period were therefore adjusted for quantitative measurements to ensure complete decay of the microwave signal.

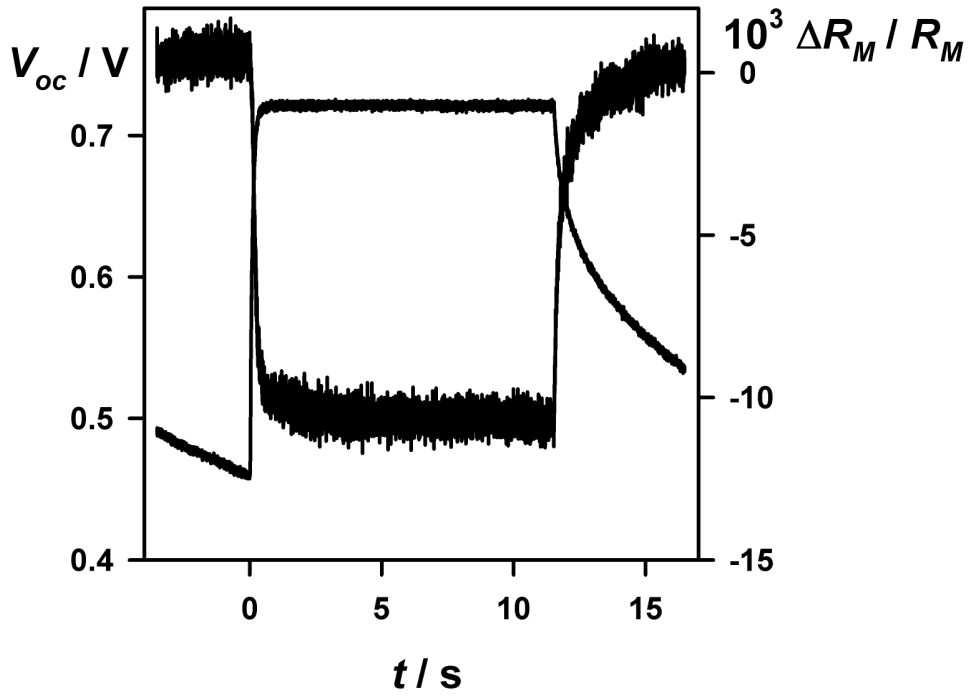

Figure 7. Normalized microwave reflectance change (negative change) and photovoltage (positive change) responses of the DSC to chopped illumination measured simultaneously. Incident photon flux (530 nm) 10^{21} $m^{-2}s^{-1}$.

The experiment illustrated in Figure 7 was repeated for a range of light intensities to obtain the dependence of $\Delta R_M/R_M$ on V_{oc} for different light intensities. The results are displayed in Figure 8. It is immediately apparent that the semilogarithmic plot of $\Delta R_M/R_M$ vs. V_{oc} does not have the slope expected for free electrons (16.8 V^{-1}). Furthermore, the large reflectance response observed at low voltages, where the free electron density is low, suggests that the microwave response is mainly related to changes in the trapped electron concentration, which is much higher than the free electron concentration at all voltages.

Theoretical microwave reflectance plots were obtained from the perturbation of the permittivity by using the stack model described in the Supporting Information. The fitting of the experimental reflectance plot involved varying the electron mobility for fixed m^*/m_e =1 and following the procedures outlined above to determine the contribution from free and trapped electrons. A good fit to the experimental microwave reflectance data was obtained for a mobility of 10^{-5} m^2 V^{-1} s^{-1}, which

corresponds to a value of $E_C - E_{F,redox}$ = 0.85 V. The predicted reflectance change is shown in Figure 8 together with the reflectance changes calculated for free and only trapped electrons alone (plots calculated for other mobility values are given in the Supporting Information). It can be seen that the contribution of free electrons only becomes measurable at the open circuit voltages above 0.7 V, when the electron quasi Fermi level approaches the conduction band.

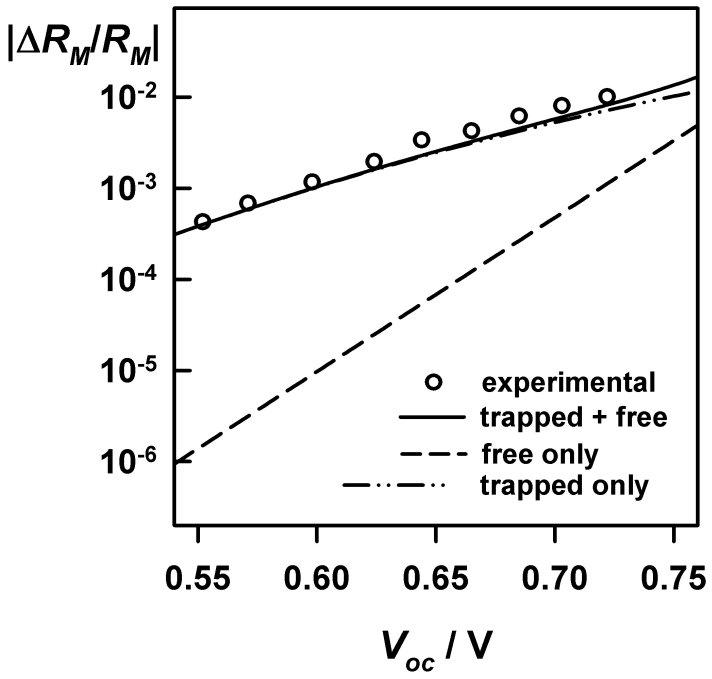

Figure 8. Fitting of the measured (negative) microwave reflectance to the response calculated for free and trapped electrons. Values used in the calculation: m^*/m_e =1, electron mobility = 10^{-5} m^2 V^{-1} s^{-1}, $E_C - E_{F,redox}$ = 0.85 V (plots calculated for other mobility values are given in the Supporting Information). The responses calculated for free and trapped electrons alone are also shown. Note that the experimental response is dominated by trapped electrons over the entire voltage range studied.

The electron mobility obtained by fitting the microwave data as described above is two orders of magnitude lower than the room temperature Hall mobility of bulk crystalline anatase TiO_2 (ca. 2×10^{-3} m^2 V^{-1} s^{-1}) reported by Forro et al.[56], but is identical to the value reported for THz measurements on sensitized mesoporous TiO_2 by Tiwana et al.[59,60] Values ranging from 10^{-6} m^2 V^{-1} s^{-1} [61] to 1.5×10^{-3} m^2 V^{-1} s^{-1} [62] have been reported for the THz electron mobility in mesoporous TiO_2, and Kroeze et al.[41] have estimated the microwave electron mobility of mesoporous anatase at 9 GHz to be 3.4×10^{-6} m^2 V^{-1} s^{-1}, which is close to the value found in the present work. However, in all these reported measurements, no

electrolyte was present and it was assumed that the responses were due to free electrons. It is worth remarking that such low values of electron mobility correspond to electron mean free paths that are smaller than the lattice constant if $m^*/m_e = 1$, which leads to problems of interpretation in terms of conventional kinetic theory, so the result may indicate that $m^*/m_e > 1$ (as noted above, the microwave reflectance is very insensitive to m^*/m_e). This could indicate strong coupling of electron motion with fluctuations of dipoles and ions in the adjacent electrolyte phase in addition to deformations of the crystal lattice.

Measurements using intensity modulated illumination

So far the discussion has been limited to the steady state microwave response of the DSC. Various transient and periodic methods are commonly used to characterize DSCs.[49] One such technique is intensity-modulated photovoltage spectroscopy (IMVS), which measures the frequency-dependent photovoltage response to small amplitude modulation of the illumination intensity. In essence, IMVS measures the relaxation of the free electron concentration by trapping/detrapping and by electron transfer ('back reaction') to I_3^-, since the free electron concentration and open circuit voltage are related by equation 6. The inverse of the characteristic relaxation frequency observed in IMVS is usually referred to as the (apparent) electron lifetime, τ_n, (note that these 'electron lifetimes' should not be confused with the momentum relaxation time, τ, employed in section II.1). Bisquert and Vikhrenko[34] have shown that the time-dependent concentrations of free and trapped electrons in the DSC are related by the quasi-static relationship

$$\frac{\partial n_t}{\partial t} = \frac{\partial n_t}{\partial n_c}\frac{\partial n_c}{\partial t} \tag{13}$$

This means that the free and trapped electron concentrations will both vary periodically under sinusoidally modulated illumination. This modulation of electron density should be detectable by microwave reflectance. An interesting point is that the time constant, τ_{IMVS}, of the IMVS response should correspond to therelaxation of free electrons, whereas the time constant, τ_M, of the microwave

response should correspond to relaxation of trapped electrons, since the results above show that these dominate the microwave response. In fact, the two time constants should be of the same order of magnitude, since at any given value of open circuit voltage, they should be related by (see Supporting Information)

$$\frac{\tau_{IMVS}}{\tau_M} = \frac{T_0}{T} \tag{14}$$

The relaxation of trapped electrons in the DSC has been characterized previously using frequency resolved near-IR measurements,[29] but the present measurement is the first example of the application of light-modulated microwave reflectance[13-15,50,63] to the DSC (see Supporting information for experimental setup). Ideally, the measurement should be made with a small amplitude modulation of the steady state light intensity in order to allow linearization of the response. Unfortunately, the signal to noise ratio in the microwave measurements was not adequate for small intensity perturbations, so 100% depth modulation was used. The lock-in amplifier then measures the first harmonic of the Fourier series representing the non-linear response. Figure 9 illustrates the semicircular frequency- resolved microwave reflectance response that was measured.

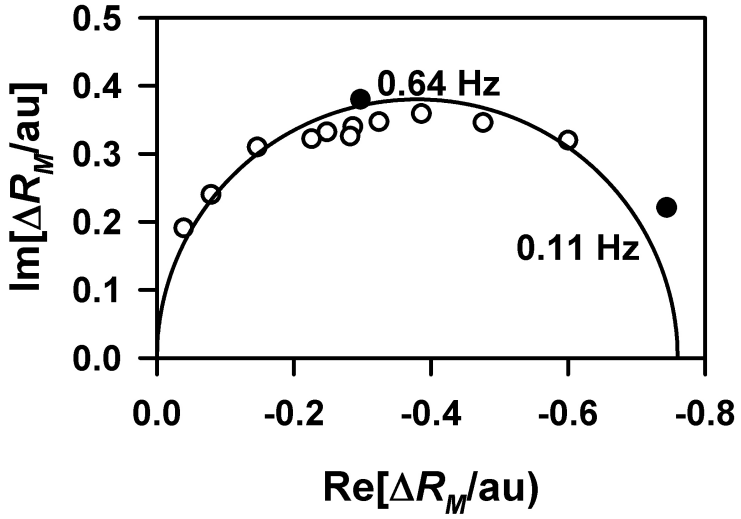

Figure 9. Intensity-modulated microwave reflectance response of DSC. Illumination 532 nm, peak incident photon flux 10^{20} m^{-2} s^{-1}. V_{oc} = 0.676 V.

In the present case, a value of T_0 = 993 K was obtained from the near-IR absorbance measurements (cf. Figure 6), so we would expect the ratio of lifetimes in equation 14 to be 3.3. In order to compare the electron lifetimes measured by IMVS and microwave reflectance, IMVS measurements were also carried out on a nominally identical cell, without the etched windows, using 100% intensity modulation. Figure 10 compares the apparent electron lifetimes derived from IMVS measurements with those obtained by the intensity-modulated microwave technique. Unfortunately since two different - although nominally identical - cells were used for the IMVS and microwave measurements and since the signal to noise ratio was poor, it was not possible to confirm that the ratio τ_{IMVS}/τ_M = 993K/298K = 3.3 as predicted. Nevertheless the lifetimes determined by the two methods are very similar, confirming that the free and trapped electron populations remain in quasi-equilibrium on the time scale of the relaxation via electron transfer to I_3^- ions in the electrolyte.

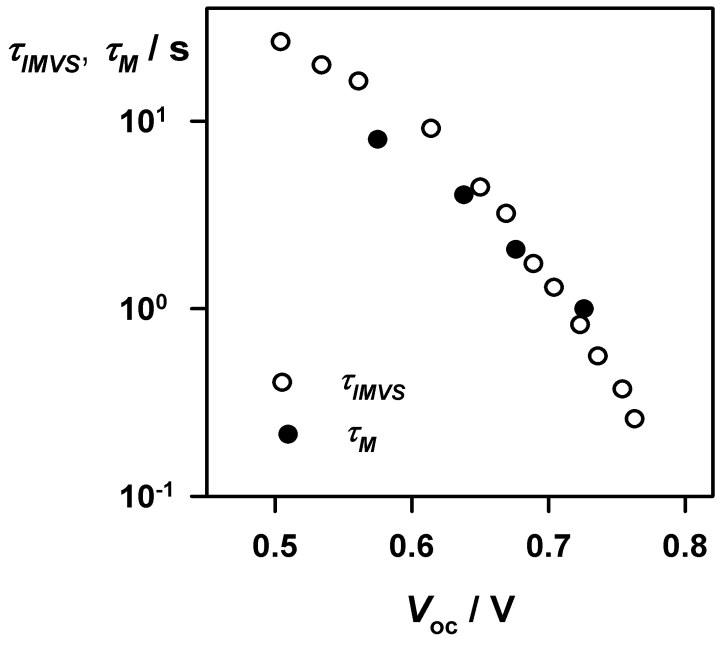

Figure 10. Comparison of the relaxation time constants obtained by IMVS and intensity-modulated microwave reflectance on two nominally identical cells (apart from removal of FTO layer for microwave measurement). In both cases, 100% depth modulation was used.

Consequences for TRMC (reflectance) measurements on DSCs

The results presented in this paper may have implications for the analysis of TRMC measurements on DSCs. TRMC measurements usually involve large amplitude perturbations, and the microwave decay is often fitted with a stretched exponential, assuming that the normalized reflectance change is linearly proportional to the change in free electron concentration. In the case of the DSC, however, it appears that TRMC measurements made with an electrolyte-filled DSC would primarily detect the decay in the *trapped* electron concentration, particularly at the low pulse energies that give injected electron densities relevant to device operation. It is therefore interesting to establish the relationship between $\Delta R_M/R_M$ and the trapped electron density in this case. Figure 11 illustrates the experimentally measured relationship between the microwave reflectance change and the increase in trapped electron concentration caused by illumination (determined by near-IR absorbance). It can be seen that the plot is non-linear. This is because the rates of decay of free and trapped electron concentrations are related by equation 13, provided that the quasistatic condition holds on the time scale of the measurements (i.e. trapping/detrapping is fast so that free and trapped electrons remain in quasi-equilibrium). The non-linearity arises from the $\partial n_t / \partial n_c$ term in equation 13, since n_t varies more slowly with voltage than n_c because $T_0 > T$.

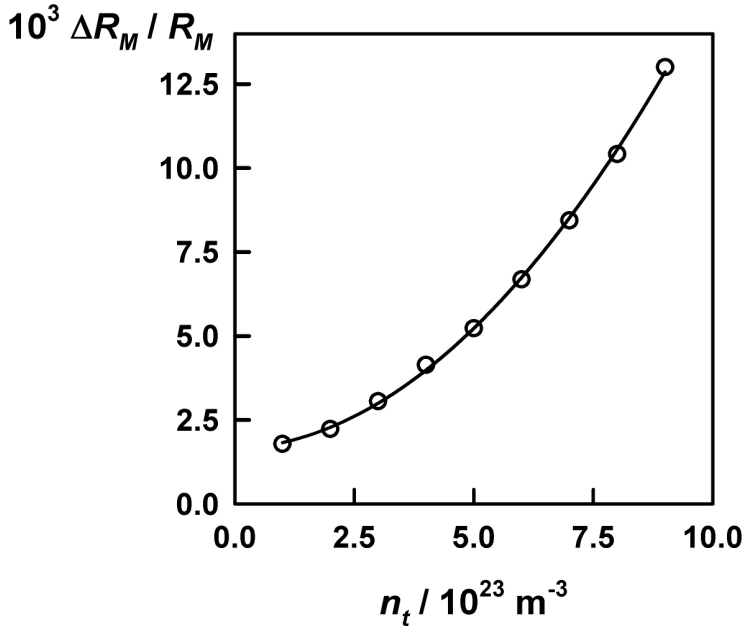

Figure 11. Experimental relationship between the light-induced change in microwave reflectance of the DSC and the corresponding change in trapped electron concentration measured by near-IR absorbance.

The existence of this non-linearity would not be easy to deduce from large amplitude perturbation measurements, where the decay of the microwave signal is non-exponential. The situation for ultrafast measurements is likely to be more complicated, since in many of these measurements the free electron concentration is much higher and the quasi-static relationship between free and trapped electron concentrations may no longer hold.

CONCLUSIONS

This study has shown that the magnitude and voltage-dependence of the light-induced microwave reflectance change measured on working DSCs cannot be understood simply in terms of changes in the conductivity of the TiO_2. It is clearly necessary to take account of the dominant influence of trapped electrons on the complex permittivity of the oxide. The experimental data can be fitted quite well using a simple harmonic oscillator to predict the dominant change in permittivity arising from trapped electrons. Although the simple harmonic model for trapped electrons is an approximation, it suffices to show that it is necessary to take trapped electrons into account in the interpretation of microwave reflectance measurements in systems in which significant electron (or hole) trapping takes place.

Acknowledgments

This work was supported by EPSRC, the University of Bath and The Ford Foundation. Impedance measurements were carried out in Uppsala by kind permission of Anders Hagfeldt. The authors acknowledge Marinus Kunst (Helmholtz Zentrum Berlin) for useful discussions, Daniel Vanmaekelbergh (Debye Institute, Utrecht) for pointing out the need to consider changes in the real component of permittivity, as well as Hynek Němec (Institute of Physics, Academy of Sciences of the Czech Republic, Prague) and Tom Savenije (Delft University of Technology) for a critical reading of earlier versions of the manuscript and helpful discussions.

Supporting Information Available. Details of the Ka-band microwave set-up and dielectric stack modeling of microwave reflectance. Information on 2-D model to simulate leakage of microwaves. Details of impedance measurements and fitting. Further details of modeling of perturbation of microwave permittivity by trapped electrons. Derivation of equation 9. Further details of the effects of electron mobility on calculated microwave reflectance response. Derivation of equation 14. This information is available free of charge via the Internet at http://pubs.acs.org.

References

(1) Peter, L. M. *J. Phys. Chem. Lett.* **2011**, *2*, 1861-1867.
(2) O'Regan, B.; Grätzel, M. *Nature* **1991**, *353*, 737-740.
(3) Peter, L. M. *J. Phys. Chem. C* **2007**, *111*, 6601-6612.
(4) Peter, L. M. *PCCP* **2007**, *9*, 2630-2642.
(5) Kunst, M.; Beck, G. *J. Appl. Phys.* **1986**, *60*, 3558-3566.
(6) Bogomolni, R. A.; Tributsch, H.; Petermann, G.; Klein, M. P. *J. Chem. Phys.* **1983**, *78*, 2578-2584.
(7) Deb, S.; Nag, B. R. *J. Appl. Phys.* **1962**, *33*, 1604-1606
(8) Kunst, M.; Beck, G.; Tributsch, H. *J. Electrochem. Soc.* **1984**, *131*, 954-956.
(9) Schlichthörl, G.; Peter, L. M. *J. Electroanal. Chem.* **1995**, *381*, 55-61.
(10) Schlichthörl, G.; Peter, L. M. *J. Electrochem. Soc.* **1995**, *142*, 2665-2669.
(11) Cass, M. J.; Duffy, N. W.; Kirah, K.; Peter, L. M.; Pennock, S. R.; Ushiroda, S.; Walker, A. B. *J. Electroanal. Chem.* **2002**, *538*, 191-203.
(12) Duffy, N. W.; Kirah, K.; Peter, L. M.; Ushiroda, S. *Z. Phys. Chem.* **2003**, *217*, 333-350.
(13) Cass, M. J.; Duffy, N. W.; Peter, L. M.; Pennock, S. R.; Ushiroda, S.; Walker, A. B. *J. Phys. Chem. B* **2003**, *107*, 5857-5863.
(14) Cass, M. J.; Duffy, N. W.; Peter, L. M.; Pennock, S. R.; Ushiroda, S.; Walker, A. B. *J. Phys. Chem. B* **2003**, *107*, 5864-5870.
(15) Peter, L. M.; Ushiroda, S. *J. Phys. Chem. B* **2004**, *108*, 2660-2665.
(16) Wunsch, F.; Schlichthörl, G.; Tributsch, H. *J. Phys. D* **1993**, *26*, 2041-2048.
(17) Holt, J. M.; Ferguson, A. J.; Kopidakis, N.; Larsen, B. A.; Bult, J.; Rumbles, G.; Blackburn, J. L. *Nano Lett.* **2010**, *10*, 4627-4633.
(18) Kroeze, J. E.; Savenije, T. J.; Warman, J. M. *J. Photochem.Photobiol. A* **2002**, *148*, 49-55.
(19) Kroeze, J. E.; Savenije, T. J.; Warman, J. M. *J. Am. Chem. Soc.* **2004**, *126*, 7608-7618.
(20) Katoh, R.; Huijser, A.; Hara, K.; Savenije, T. J.; Siebbeles, L. D. A. *J. Phys. Chem. C* **2007**, *111*, 10741-10746.
(21) Friedrich, D.; Kunst, M. *J. Phys. Chem. C* **2011**, *115*, 16657-16663.
(22) Salafsky, J. S.; Lubberhuizen, W. H.; vanFaassen, E.; Schropp, R. E. I. *J. Phys. Chem. B* **1998**, *102*, 766-769.
(23) Anderson, A. Y.; Barnes, P. R. F.; Durrant, J. R.; O'Regan, B. C. *J. Phys. Chem. C* **2011**, *114*, 1953-1958.
(24) Boschloo, G. K.; Goossens, A. *J. Phys. Chem.* **1996**, *100*, 19489-19494.
(25) Peter, L. M.; Ponomarev, E. A.; Franco, G.; Shaw, N. J. *Electrochim. Acta* **1999**, *45*, 549-560.
(26) Berger, T.; Anta, J. A.; Morales-Flórez, V. *J. Phys. Chem. C* **2012**, *116*, 11444-11455.
(27) Duffy, N. W.; Peter, L. M.; Rajapakse, R. M. G.; Wijayantha, K. G. U. *Electrochem. Commun.* **2000**, *2*, 658-662.
(28) Bailes, M.; Cameron, P. J.; Lobato, K.; Peter, L. M. *J. Phys. Chem. B* **2005**, *109*, 15429-15435.
(29) Franco, G.; Gehring, J.; Peter, L. M.; Ponomarev, E. A.; Uhlendorf, I. *J. Phys. Chem. B* **1999**, *103*, 692-698.
(30) Nguyen, T. T. O.; Peter, L. M.; Wang, H. X. *J. Phys. Chem. C* **2009**, *113*, 8532-8536.
(31) Zhu, K.; Schiff, E. A.; Park, N. G.; van de Lagemaat, J.; Frank, A. J. *Appl. Phys. Lett.* **2002**, *80*, 685-687.
(32) Kopidakis, N.; Neale, N. R.; Zhu, K.; van de Lagemaat, J.; Frank, A. J. *Appl. Phys. Lett.* **2005**, *87* 20216.
(33) Nakade, S.; Saito, Y.; Kubo, W.; Kitamura, T.; Wada, Y.; Yanagida, S. *J. Phys. Chem. B* **2003**, *107*, 8607-8611.
(34) Bisquert, J.; Vikhrenko, V. S. *J. Phys. Chem. B* **2004**, *108*, 2313-2322.
(35) Kytin, V.; Porteanu, H. E.; Loginenko, O.; Dittrich, T.; Konstantinova, E.; Timoshenko, V. Y.; Koch, F.; Kashkarov, P. K. *Phys. Stat. Sol. A* **2003**, *197*, 257-262.

(36) Porteanu, H. E.; Timoshenko, V. Y.; Dittrich, T.; Koch, F. *Phys. Stat. Sol. A* **2000**, *182*, 201-206.
(37) Grabtchak, S.; Cocivera, M. *Phys. Rev. B* **1998**, *58*, 4701-4707.
(38) Porteanu, H. E.; Konstantinova, E.; Kytin, V.; Loginenko, O.; Timoshenko, V.; Dittrich, T.; Koch, F. In *Electrically Based Microstructural Characterization Iii*; Gerhardt, R. A. W. A. P. A. M. A. C. G. M., Ed. 2002; Vol. 699, p 251.
(39) Wetzelaer, G. A. H.; Koster, L. J. A.; Blom, P. W. M. *Phys. Rev. Lett.* **2011**, *107*, 066605.
(40) Hartwig, W. H.; Hinds, J. J. *J. Appl. Phys.* **1969**, *40*, 2020-2027.
(41) Lobato, K.; Peter, L. M. *J. Phys. Chem. B* **2006**, *110*, 21920-21923.
(42) van Faassen, E. *Phys. Rev. B* **1998**, *58*, 15729-15735.
(43) Nemec, H.; Kuzel, P.; Sundstrom, V. *J. Photochem. Photobiol.A* **2010**, *215*, 123-139.
(44) Vanzura, E. J.; Bakerjarvis, J. R.; Grosvenor, J. H.; Janezic, M. D. *Ieee Trans. Microwave Theory and Techniques* **1994**, *42*, 2063-2070.
(45) Jin, F.; Tong, H.; Shen, L.; Wang, K.; Chu, P. K. *Mater. Chem. Phys.* **2006**, *100*, 31-33.
(46) Barthel, J.; Buchner, R.; Eberspacher, P. N.; Munsterer, M.; Stauber, J.; Wurm, B. *J. Mol. Liq.* **1998**, *78*, 83-109.
(47) Rubinger, C. P. L.; da Cunha, A. F.; Vinagre, F.; Ribeiro, G. M.; Costa, L. C. *J. Appl. Phys.* **2009**, *105* 074502.
(48) Fabregat-Santiago, F.; Garcia-Belmonte, G.; Bisquert, J.; Zaban, A.; Salvador, P. *J. Phys. Chem. B* **2002**, *106*, 334-339.
(49) Hagfeldt, A.; Peter, L. M. In *Dye Sensitized Solar Cells*; Kalyanasundaranam, K., Ed.; EPFL Press: Lausanne, 2010, pp 323-402.
(50) Schlichthörl, G.; Ponomarev, E. A.; Peter, L. M. *J. Electrochem. Soc.* **1995**, *142*, 3062-3067.
(51) Wang, H. X.; Peter, L. A. *J. Phys. Chem. C* **2009**, *113*, 18125-18133.
(52) Dunn, H. K.; Westin, P.-O.; Staff, D. R.; Peter, L. M.; Waker, A. B.; Boschloo, G.; Hagfeldt, A. *J. Phys. Chem. C* **2011**, *115*, 13932-13937.
(53) Tang, H.; Prasad, K.; Sanjines, R.; Schmid, P. E.; Levy, F. *J. Appl. Phys.* **1994**, *75*, 2042-2047.
(54) Enright, B.; Fitzmaurice, D. *J. Phys. Chem.* **1996**, *100*, 1027-1035.
(55) Huynh Anh, H.; Aradi, B.; Frauenheim, T.; Deak, P. *Phys. Rev. B* **2011**, *83* 155201
(56) Forro, L.; Chauvet, O.; Emin, D.; Zuppiroli, L.; Berger, H.; Lévy, F. *J. Appl. Phys.* **1994**, *75*, 633-635.
(57) Cameron, P. J.; Peter, L. M.; Hore, S. *J. Phys. Chem. B* **2005**, *109*, 930-936.
(58) Cameron, P. J.; Peter, L. M. *J. Phys. Chem. B* **2005**, *109*, 7392-7398.
(59) Tiwana, P.; Parkinson, P.; Johnston, M. B.; Snaith, H. J.; Herz, L. M. *J. Phys. Chem. C* **2010**, *114*, 1365-1371.
(60) Tiwana, P.; Docampo, P.; Johnston, M. B.; Snaith, H. J.; Herz, L. M. *Acs Nano* **2011**, *5*, 5158-5166.
(61) Hendry, E.; Wang, F.; Shan, J.; Heinz, T. F.; Bonn, M. *Phys. Rev. B* **2004**, *69* 081101.
(62) Turner, G. M.; Beard, M. C.; Schmuttenmaer, C. A. *J. Phys. Chem. B* **2002**, *106*, 11716-11719.
(63) Schlichthörl, G.; Ponomarev, E. A.; Peter, L. M. *J. Electrochem. Soc.* **1995**, *142*, 3062-3067.

TOC